



Turkish Earthquake Foundation - Earthquake Engineering Committee  
Prime Ministry, Disaster And Emergency Management Presidency

## STUDY ON SEISMIC VULNERABILITY EVALUATION OF AN OHS FACILITY

G.C. Yao<sup>1</sup>, W.C. Chen<sup>2</sup>, W.J. Chou<sup>3</sup>, Y.C. Chang<sup>4</sup>

### ABSTRACT

Considering efficiency of product transportation and space saving, suspended overhead material handling system (OHS) has become an essential transportation facility in high-tech factories in Taiwan. This suspended system swings easily during earthquakes and shut down the whole production line when its deformation exceeds limit criteria in earthquakes. Therefore slender threaded bars are installed as lateral braces to resist earthquake force by engineering judgement only. This study investigates the seismic capacity of an OHS system in the cleanroom of a high-tech factory of such condition and attempts to improve its performance through full-scale experiments and computer analysis.

Full-scale specimens of the OHS were tested with static lateral cyclic loading, and the damage patterns were observed during each displacement level following FEMA-461. Details about the failure modes and the stiffness degradation were interpreted in this study. SAP2000 was used to build a computer model based on the experiment data and the nonlinear pushover analysis was performed. This study also tested the dynamic cyclic behavior of the braces, and defined the hysteresis loop of the braces in the computer model. The computer model then was subjected to cyclic dynamic loading to simulate building floor responses in an earthquake. The analysis result showed the internal force distribution of the system, and estimated the peak excitation floor acceleration when the OHS reached the limit displacement. A retrofit program was proposed based upon the dynamic analysis and could efficiently increase system strength to the designed bracing strength. Most important of all, the proposed retrofit program was economical and practical and could be constructed in-situ quickly and easily.

### INTRODUCTION

For the efficiency of product transportation, many high-tech factories place the material-transportation cars suspended on the overhead space so as to avoid complex equipments layout and employee circulation on the floor. Figure 1 shows the suspended overhead material handling system (OHS) in the cleanroom of a high-tech factory in Taiwan. The construction of the OHS is basically identical but with differences on suspension system. Rods ( $\phi 5/8$ " ) are common material used to suspend the OHS, and are fastened to the building structure with clamps and bolts since welding is not

<sup>1</sup> Professor, Department of Architecture, National Cheng Kung University, Tainan, Taiwan

<sup>2</sup> Ph. D. Student, Department of Architecture, National Cheng Kung University, Tainan, Taiwan

<sup>3</sup> Graduate Student, Dept. of Architecture, National Cheng Kung University, Tainan, Taiwan

<sup>4</sup> Graduate Student, Dept. of Architecture, National Cheng Kung University, Tainan, Taiwan

permitted in an operating cleanroom. Because the suspension length of the OHS is usually more than three meters, this suspended system swings easily during earthquakes and results in significant displacement. In order to solve this problem, slender threaded bars ( $\phi 3/8"$ ) are often used as lateral braces to resist the earthquake force by judgement. But according to previous earthquake experiences, this method reduces the displacement inefficiently.

This paper aims at identifying the seismic capacity of an OHS system. Through full-scale experiments, damage patterns of this system are observed and a computer model is subsequently built based on the experiment data. This computer model not only shows clearly the internal force distribution of the system but also provides the displacement analysis with reliable accuracy. In addition to the static lateral loading tests, dynamic cyclic tests of the braces are studied as well in this paper. According to the experiment results and the computer analysis, the critical problems of the OHS are indicated and thus a retrofit program is proposed.

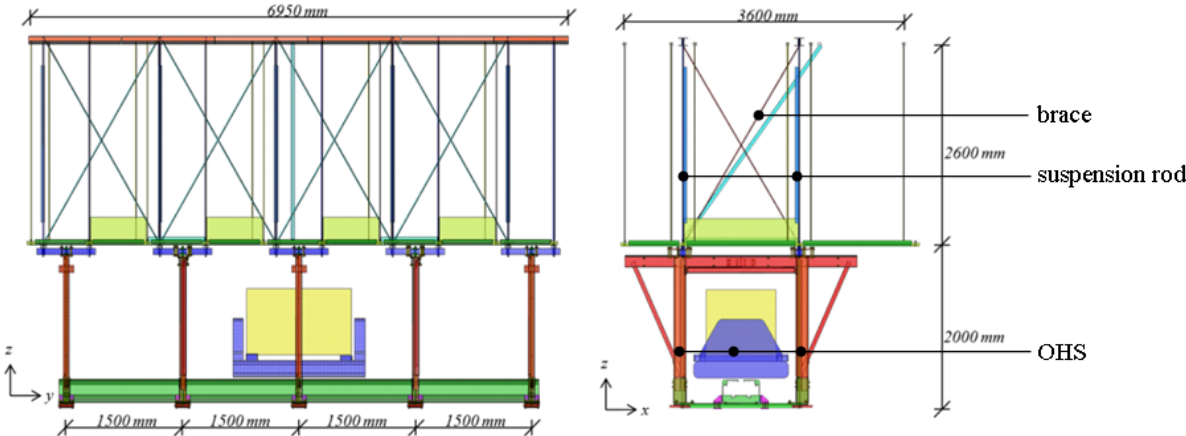


Figure 1. Suspended overhead material handling system (OHS) with suspension rod and brace

**FULL-SCALE EXPERIMENTAL PROGRAM**

Figure 2 shows the in-situ condition of the OHS in a high-tech factory. The main construction includes the hanging frames and an aluminum rail supporting the moving cars. Sometimes the hanging frames maybe supported by braced frames to increase the structural stiffness. Basically, the hanging frames are directly connected to the building structure. But since the floor height is usually over ten meters above the operation floor, therefore, many long and slender suspension rods shown in Figure 1 are applied to connect the OHS to the building. In Figure 2, the OHS is shown connected to the ceiling only. But in reality, the OHS and the ceiling are seperated and have their independent suspension systems from building structures above the ceiling. Figure 3 shows the schematic OHS supporting system where the suspension rods from the building structure extend through the ceiling to support the OHS system.

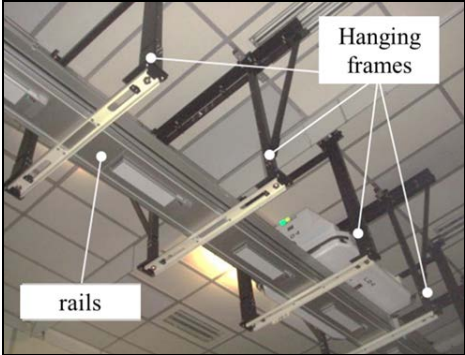


Figure 2. OHS photos in a high-tech factory

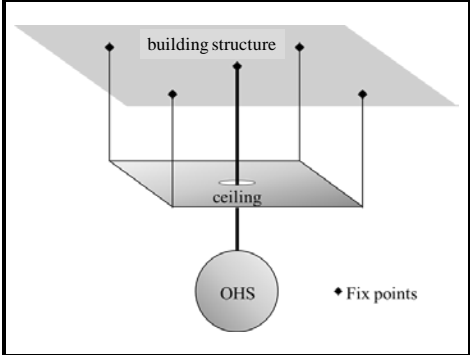


Figure 3. Schematic OHS supporting

Figure 4 shows a full-scale specimen of the OHS system constructed in this study. The huge steel frames serve as building structures, and for the sake of reality, the ceiling system is also added in the specimens together. The total height of the specimen including two parts is about 4600mm, the OHS is 2000mm tall while the suspension rod is 2600mm (Fig.1). To avoid producing extra torsion during testing, the specimen is designed symmetrically with five sets of hanging frames, and the lateral loading is applied to the central hanging frame of the system (Fig.5). The spacing of each hanging frame is 1500mm which makes the OHS 6000mm long. Among the hanging frames, the second and the fourth ones are supported by braced frames. Each hanging frame is hung by four suspension rods ( $\phi 5/8$ ") and all the rods are fastened to the OHS and the steel frames with clamps and bolts. Some of the suspension rods are reinforced with C channel (50\*50\*2\* 2000mm) shown in Figure 5. Details of all connections strictly follow the in-situ conditions. Besides, slender threaded bars ( $\phi 3/8$ ") are installed as lateral braces above the second and the fourth hanging frames.



Figure 4. Full-scale specimen of OHS

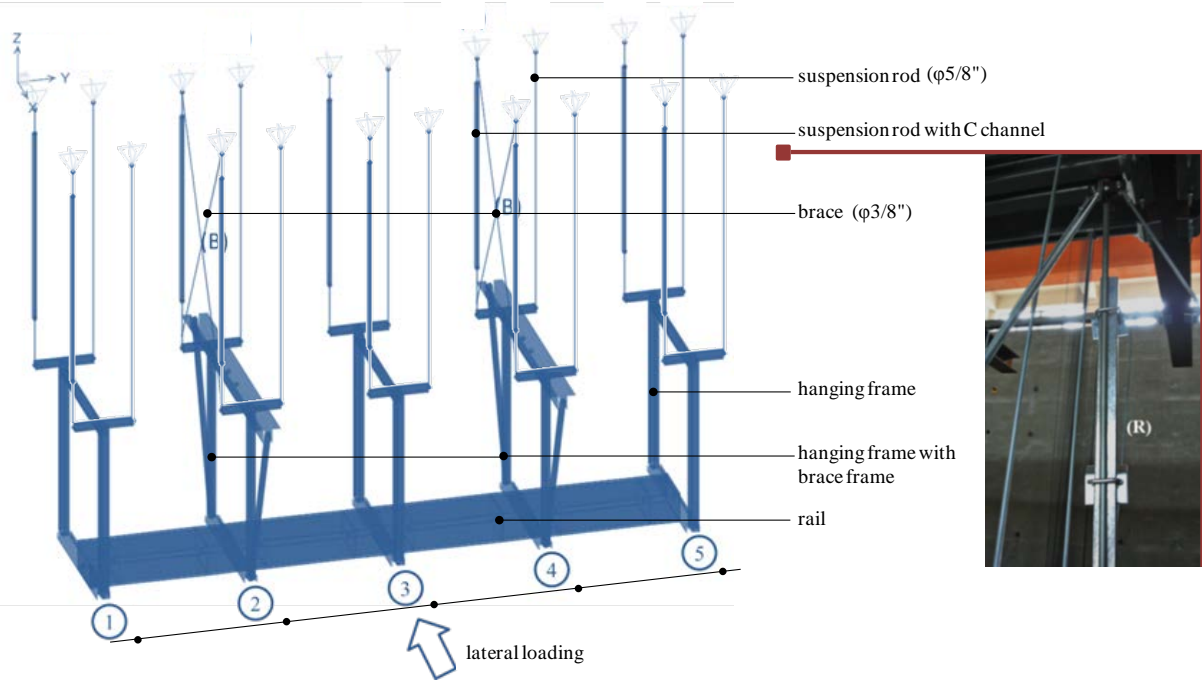


Figure 5. Details of the OHS specimen

The OHS is tested in an experimental program that FEMA-461 [1] recommends for the investigation of the seismic performance of nonstructural components. The actuator is displacement controlled with the velocity of 1.38mm/sec, and 10 different stages are tested in sequence, with the

increase of the displacement by 40% each time. The first stage is tested with six loops, and the rest of the stages are tested with two loops. The damage conditions are investigated and recorded during each stage until any one of the components detached from the specimen or is about to rupture.

**EXPERIMENT RESULT**

Some typical damage patterns of the current OHS system were revealed in the first experiment. Failure happened mainly on the connections especially between the suspension rod and the structure where the clamps visibly slid (Fig.6). With increasing displacement, connections between the rod and the OHS were damaged gradually (Fig.7), and this situation happened not only on the suspension rods but also on the braces. In addition, the connecting plates of the braces were damaged seriously (Fig.8) and the suspension rods were observed buckled (Fig.9) at the end of the experiment.



Figure 6. Sliding of the clamp

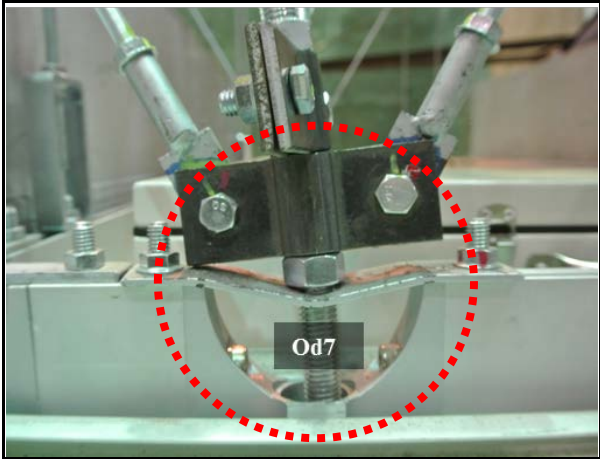


Figure 7. Failure on the connection



Figure 8. Fracture of the connecting plate

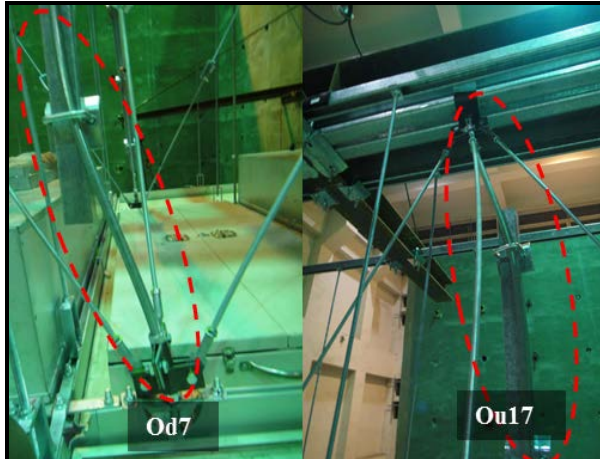


Figure 9. Buckling of the suspension rod

The first experiment showed clearly what happened to the OHS under small excitation, and the system failed before braces can provide major resistance. Apparently the OHS relied on braces to resist the lateral force during earthquakes; however, the premature loosening of the connections took place before the braces could provide designed strength. The descending slope in Figure 10(a) exhibits the degrading stiffness of the system in cyclic loadings caused by the loosening of the connections. In order to make the brace system function normally to resist the lateral loading, some vulnerable connections were reinforced and the thickness of the connecting plates were also increased in the second experiment. Figure 11 demonstrates the reinforced clamp fastening the suspension rod to the structure.

The second experiment was conducted after the connection problems were improved. It was terminated with many suspension rods buckled and a great lateral deformation exhibited. Figure 10(b) shows the force-displacement diagram in this experiment. In comparison with the first test, the stiffness decay problem was improved after reinforcing the local attachments. Most important of all, the residual displacement after every loading stage has reduced greatly, which is of particular concern in a precision production line. Figure 12 compares the residual displacement between experiment 1 and 2 from stage 5 to stage 10, since the residual displacement is similar before stage 5.

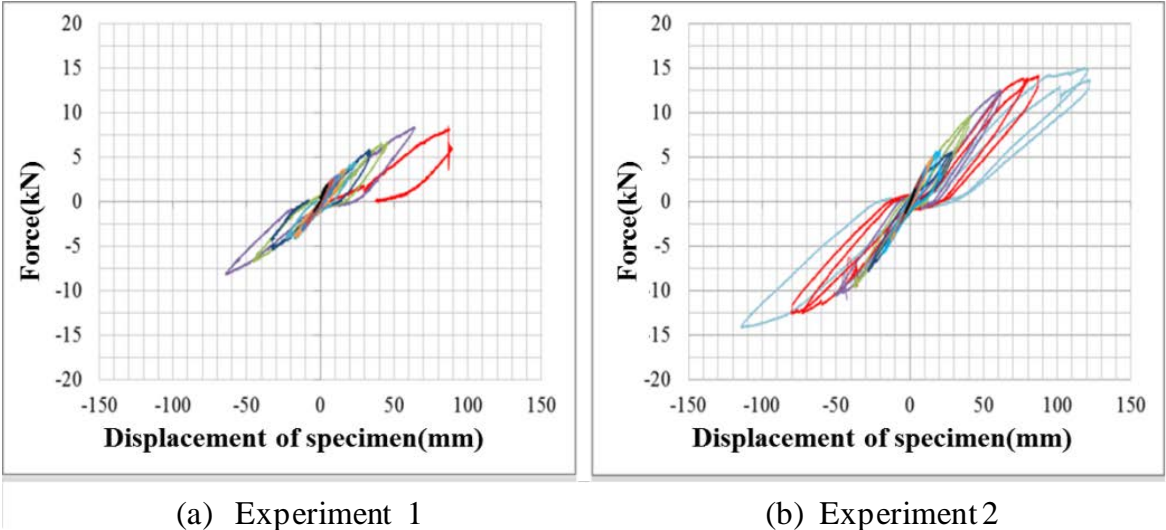


Figure 10. Force-displacement diagram of experiment 1 and experiment 2

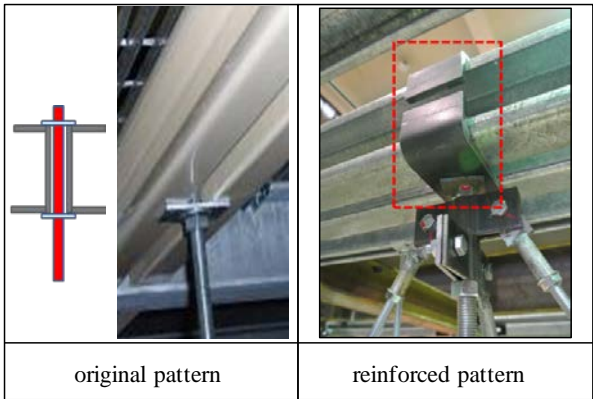


Figure 11. Reinforcement of the clamp

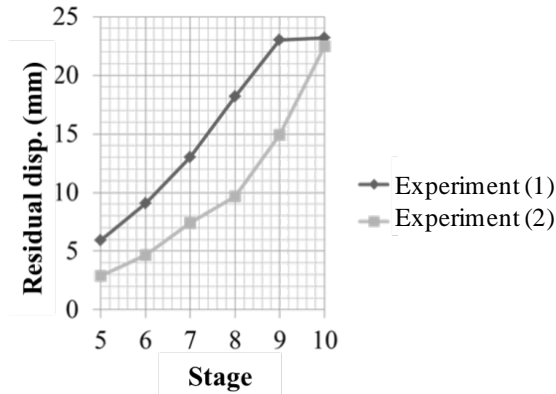


Figure 12. Comparison of residual displacement

**COMPUTER MODEL STATIC ANALYSIS**

Structural analysis software, SAP2000, was used to generate a computer model. All the setting included material property, frame section property, boundary condition, and the loading followed the testing specimen. Since there were many slender elements in the OHS which could easily buckle, the nonlinear pushover analysis was performed. The plastic hinge was defined by axial force, shear force or moment. Because the elements with high slenderness ratio behaved like two force members, tension limit and compression limit were adopted in the frame property designation. A finished computer model is showed in Figure 13. Based on the experiment data of relation between force and displacement, the validity of the computer model was proven by exhibiting the same stiffness as that in Figure 10(b). Figure 14 displays the capacity curve of the computer model in comparison with the experiment results, and it shows that the envelope curve matches the experiment curve well.

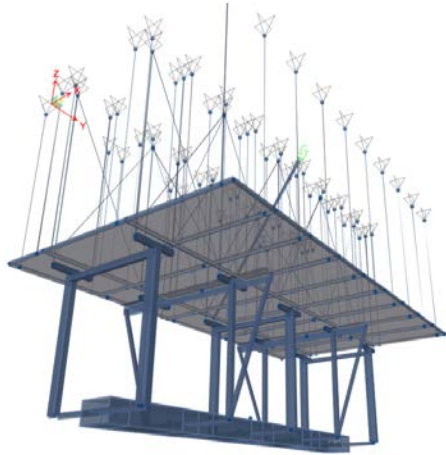


Figure 13. OHS computer model

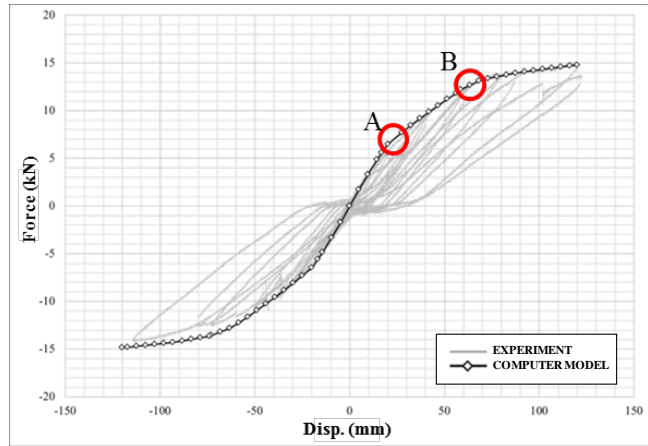


Figure 14. Capacity curve of computer model and experiment

In Figure 14, two critical points A and B where the stiffness of the envelope curve undergoes a serious reduction, are particularly worth mentioning. To understand what happened at these two points, the internal force of every single member was inspected and analyzed carefully.

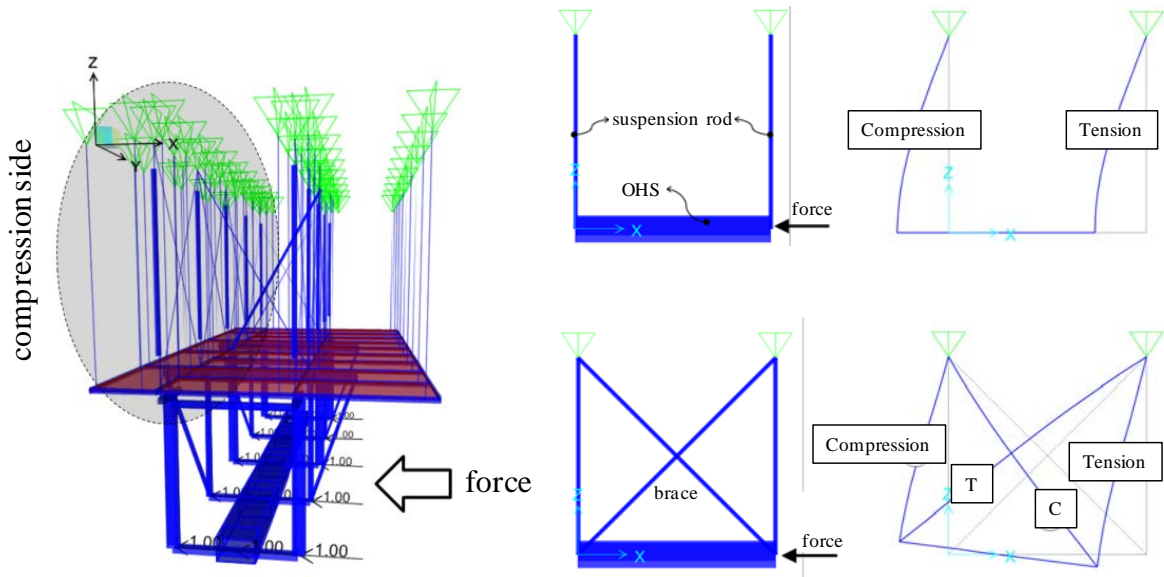


Figure 15. Axial force diagram of the suspension rods and the braces above ceiling

Shadow area in Figure 15, the suspending frames above the ceiling, is in compression when the model is subjected to a horizontal force from the right hand side. Among all the suspension rods, the ones with reinforced C channel shown in Figure 16 (No.419, No.421, No.423, No.425 and No.427) attract higher compression force than the others. Furthermore, the lateral braces above the ceiling increase the local stiffness and cause No.421 and No.425 to share the largest compression force. With the increasing of the lateral force, these two members quickly buckle almost at the same time. The first critical point A represents the compression rods reaching their buckling load which causes the system stiffness to reduce.

After the first two members buckled, the internal force of the system redistributed and the rest of the three frames (No.419, No.423 and No.427) carried more compression force. Eventually, all the members are buckled one by one; meanwhile, the stiffness of the system decreases obviously. This phenomenon is demonstrated by the second critical point B. Figure 17 compares the buckling capacity of the reinforced rods with the experiment results. It is evident that the system stiffness reduction corresponds to the buckling behavior of the suspension rods. After point B appears, the lateral resistance of the system can only depend on the slender brace and only provides small stiffness.

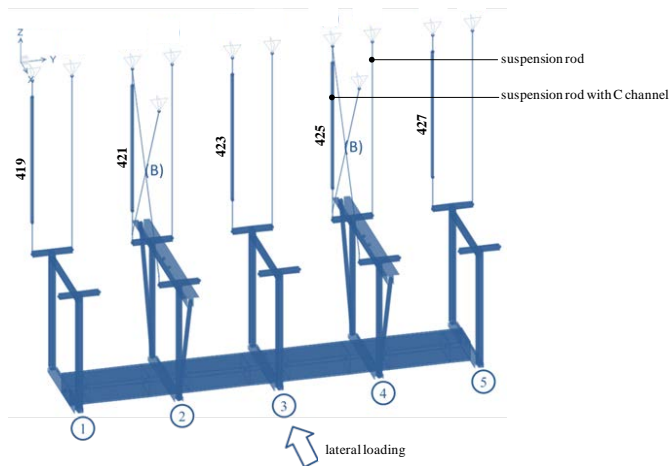


Figure 16. OHS computer model

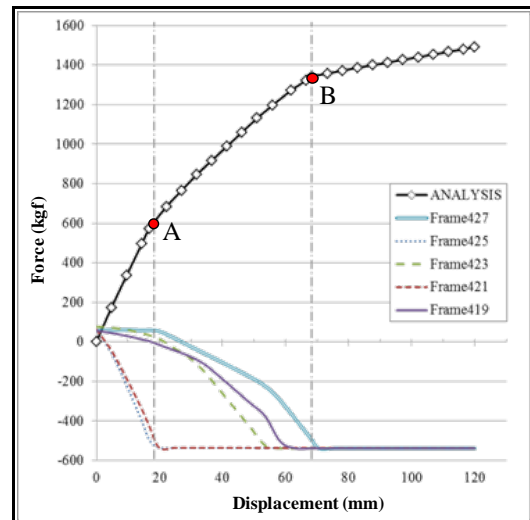


Figure 17. Diagram of buckling capacity

The computer analysis points to an important message; that is, not only the braces but also the suspension rods can help resist the lateral force through frame action. Based on this buckling-controlled behavior, increasing the buckling load of the suspension rod should be an efficient solution.

## COMPUTER MODEL DYNAMIC ANALYSIS AND RETROFIT SCHEHE

From the computer model, the OHS system has a natural frequency of 2.53 Hz close to the experiment specimen verified by using the ambient vibration experiment. The problem of the decaying stiffness represents that the system's natural frequency diminishes gradually and moves closer to the building's fundamental frequency of 1 Hz. Therefore, concerns for the resonance effect cannot be ignored. Even a little vibration may lead to large displacement by resonance and cause fatal destruction in a real earthquake condition.

Because the dynamic mechanical behavior of bars with high slenderness ratio has not been extensively studied, this paper also tested the threaded bars axially with different lengths and diameters in different excitation frequencies.

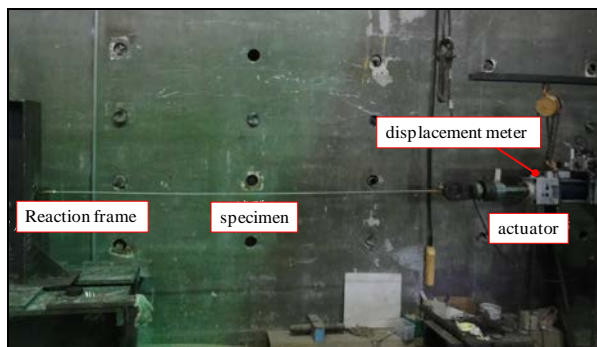


Figure 18. Dynamic cyclic experiment of slender bar

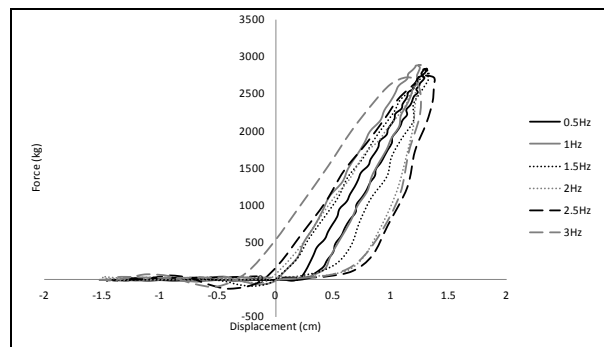


Figure 19. Hysteresis loop diagram

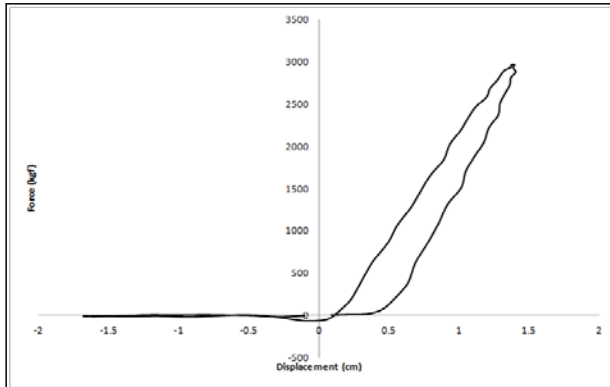
The chosen diameters of the rod specimens are 3/8" and 5/8", and their respective slenderness ratio are 1092 and 655 with length 2600mm. In order to compare specimens with the same slenderness ratio but different diameter, another  $\phi$  3/8" specimen with length of 1560mm and slenderness ratio of 655 is tested. The slender specimens are tested by using an actuator with six different exciting frequencies (0.5Hz, 1Hz, 1.5Hz, 2Hz, 2.5Hz, and 3Hz). Figure 18 displays the dynamic cyclic experiment of the slender threaded bars.

From the experiment results, it is found that influence by the slenderness ratio are not significant. The reason is that no matter how the slenderness ratio changes, the slenderness ratio is still very high for all the specimens in this study. Therefore, the specimens behave similarly without

distinct differences. But there is one thing worth noticing, the hysteresis loop of the specimen demonstrates some effects of energy dissipation capacity even at the elastic stage. And the effect increases along with the raising of exciting amplitude and frequency (Fig. 19). The result points to another important message, the bars with high slenderness ratio can dissipate energy under cyclic loading.

The Pivot Model [2] is used in the computer analysis to obtain a reasonable hysteresis loop on the basis of experiment results. Although this model is studied for reinforced concrete members, but the multi-linear plastic behavior of this model is still valuable for application in this research. Figure 20 displays a hysteresis loop of the computer model which matches the loop well in comparison with the experiment data.

hysteresis loop of the experiment



hysteresis loop of the Pivot Model

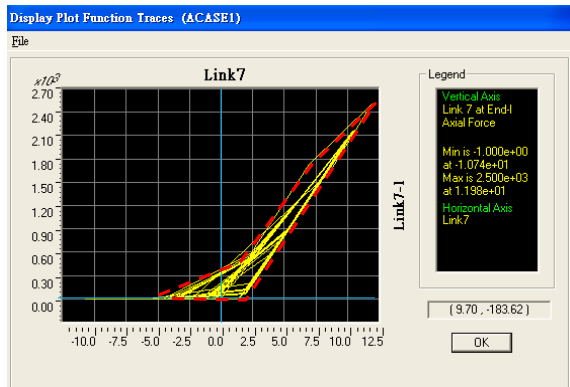


Figure 20. Hysteresis loops of the experiment and Pivot Model

The above characteristic of the hysteresis loops for the suspension rods and the braces are defined in the computer model. The computer model is then subjected to cyclic dynamic loading with different level of exciting accelerations, and the relation between displacement and acceleration can be observed. Through computer analysis, it is clearly shown how much displacement the OHS deforms with different amplitudes of exciting acceleration. Thus the point A has its corresponding exciting acceleration 125 gal while the point B is 630 gal, as shown in Figure 21. In this picture, the point B can be defined as the ultimate excitation acceleration capacity. But since the designed excitation acceleration of the OHS is 750 gal in this factory, the system needs to be reinforced.

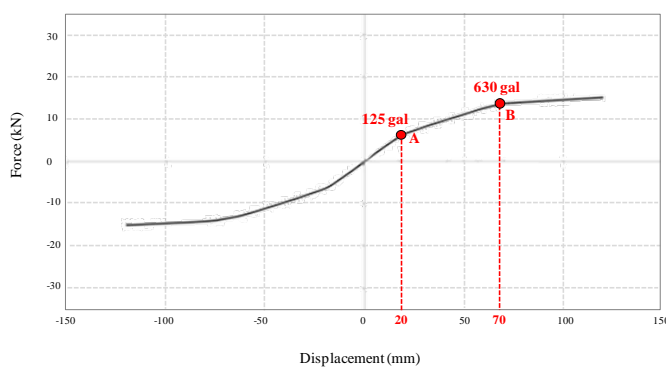


Figure 21. Exciting acceleration of point and point B

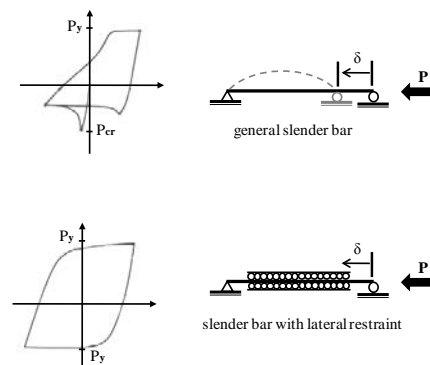


Figure 22. Schematic diagram of hysteresis loop

In addition to increasing the buckling load of the slender bars, consuming the loading energy can also raise the lateral resistance of the OHS system. On the basis of these two reasons, providing lateral restraints to the slender bars shows a great solution. For the general slender bar, the buckling strength is small and provides little energy dissipation under compression force. But the slender bar reinforced with C channels and tied with many lateral restraints, the buckling strength of the slender bar increases, which enables the member to enter yielding under compression force. This phenomenon

makes the hysteresis loop area fuller and provides better energy dissipation effects. Figure 22 compares two schematic hysteresis loop diagrams of general and restrained slender bars.

Since the C channel are used commonly in practice and also meets the requirements for convenience and workability, it is chosen to provide the lateral restraint to the slender bars in this study. With an emphasis on enhancing the buckling strength of the slender bar over the yield strength of the material, two C channels (50\*50\*2\* 2000mm) are used to restrain one slender bar. Because the yield strength of the material and the frame properties such as the section area and the moment inertia are all understood, the required length of the C channels can be calculated by the theory of the buckling load with varying dimensions [3]. Details of the retrofit scheme are shown in Figure 23.

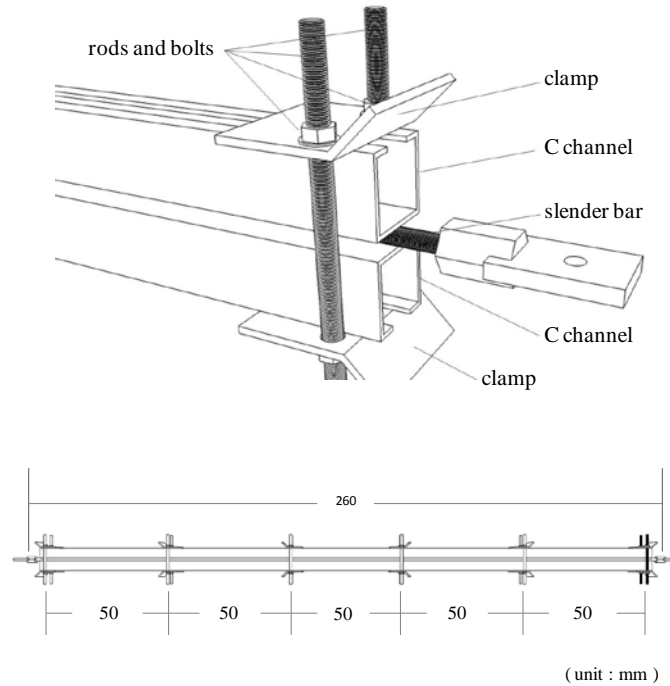
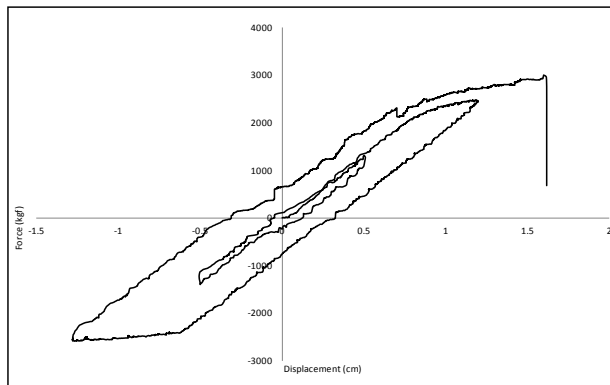


Figure 23. Details of the retrofit scheme

There were two types of slender bars in the OHS,  $\phi 3/8"$  was used for brace while  $\phi 5/8"$  was used for suspension rod. In order to find out the true hysteresis loop of the Reinforced Brace ( $\phi 3/8"+2C$ ) and the Reinforced Rod ( $\phi 5/8"+2C$ ), specimens with restraining C channels were tested with cyclic dynamic loading in this research. According to the experiment result, the Reinforced Brace demonstrated a complete hysteresis loop since the member yielded both in tension and compression. And this kind of hysteresis loop can be simulated with the Kinematic Model [2] in the computer model analysis (Fig.24).

hysteresis loop of the experiment



hysteresis loop of the Kinematic Model

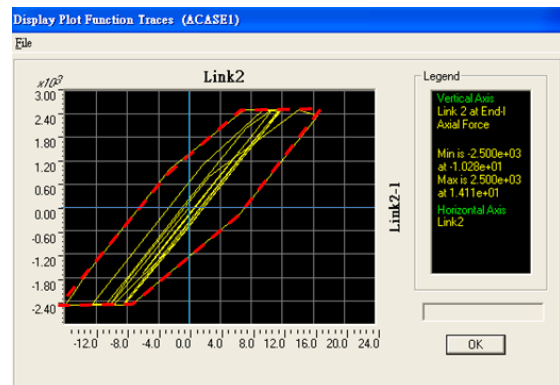
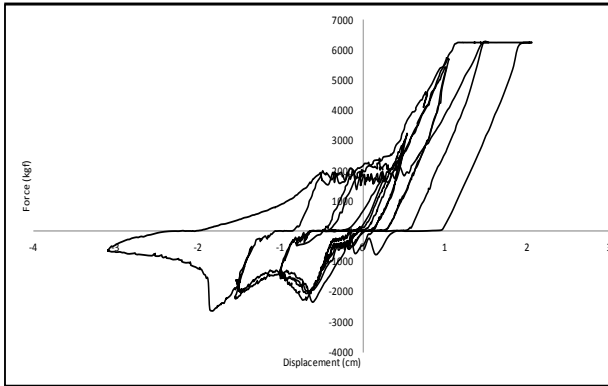


Figure 24. Hysteresis loops of the experiment and Kinematic Model

For the Reinforced Rod, the hysteresis loop (Fig.25) was incomplete and asymmetric because of damage happened on the C channels (Fig.26). The  $\phi$  5/8" rod deformed the C channels when compressed to 2500 kgf and the Reinforced Rod lost its strength to resist more compression. This type of hysteresis loop was simulated with the Pivot Model in the computer model analysis.

hysteresis loop of the experiment



hysteresis loop of the Pivot Model

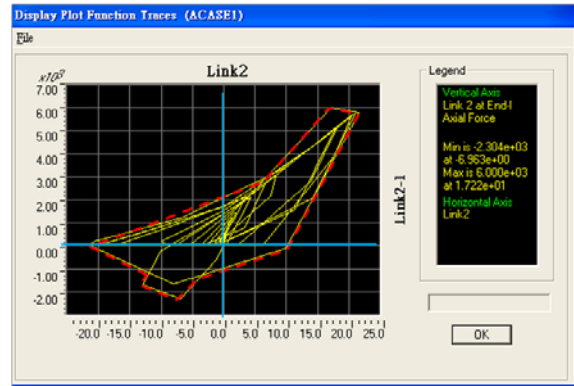


Figure 25. Hysteresis loops of the experiment and Pivot Model



Figure 26. Deformation of the C channels

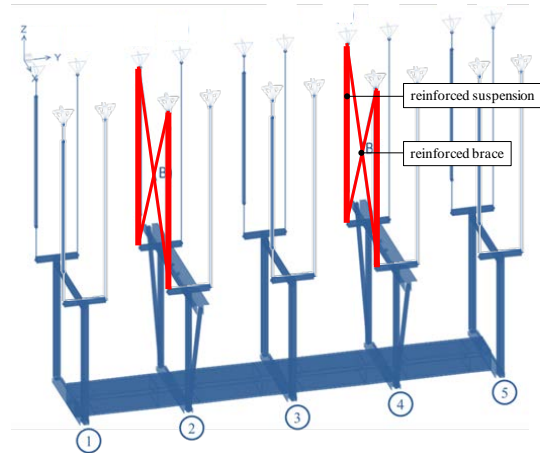


Figure 27. Locations of the reinforced components

After different types of the hysteresis loop are defined in the OHS computer model, and a retrofit system is developed. Four reinforced suspension rods and four reinforced braces take the place of the original members, and the rest of the components remains the same. Figure 27 displays the locations of the reinforced members. Through dynamic computer analysis, a new seismic capacity curve is performed (Fig.28).

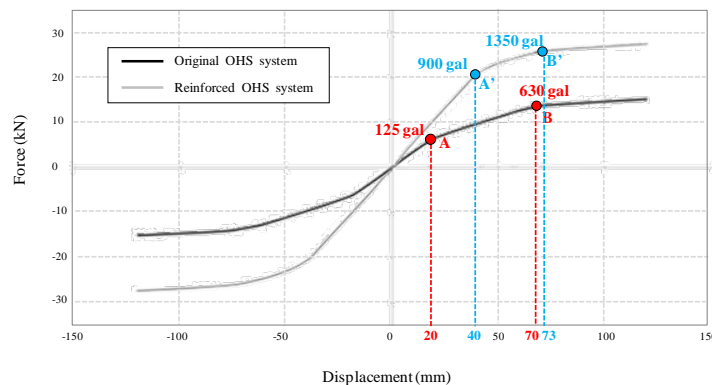


Figure 28. Details of the retrofit scheme

Comparing to the original seismic capacity curve, not only the whole new curve but also some specific points with their corresponding exciting accelerations increase significantly. In the original OHS, the stiffness of the system reduces while the excitation floor acceleration reaches 125 gal. But the stiffness of the reinforced system starts descending only when the excitation floor acceleration approaches 900 gal. Most of all, the ultimate excitation acceleration of the OHS increases from 630 gal to 1350 gal. The result shows that the modifications of the reinforced suspension rods and the braces are effective to improve the seismic capacity of the OHS.

## CONCLUSIONS

The seismic capacity of an OHS was tested, evaluated, and strengthened in this study. The loosening and damage conditions at the connections led to a instant reduction of the lateral resistance for the system in the first test. These premature failure problems happened before the braces could provide designed strength. A series of reinforced methods at the connections were developed to correct this situation.

After the connections were improved, the second test found that the lateral stiffness of the OHS still gradually decreased since the suspension rods would buckled. This phenomenon might result in resonance amplification on the OHS system. Therefore, the retrofit concept was to raise the buckling strength of the suspension rods in order to increase the seismic capacity of the OHS. It was also found that the bars with high slenderness ratio could dissipate some energy during cyclic loading after embeded in channels. This study also tested the dynamic cyclic behavior of the slender braces and defined the hysteresis loop of the braces in the computer model.

A computer model of the OHS was built based on the experiment data and was subjected to cyclic dynamic loading to simulate actual responses of the OHS system in an earthquake. The analysis estimated the excitation floor acceleration capacity when the OHS reached the limit displacement. The retrofit program was also proposed based upon the computer dynamic analysis. The reinforced system showed that the retrofit modification was an effective solution to improve the ultimate capacity of the OHS from 630 gal to 1350 gal. Most important of all, this retrofit program was economical and practical, which can be constructed in-situ quickly and easily.

## ACKNOWLEDGEMENTS

This study was supported by the National Science Council of Taiwan under Grant No. 301204402. The authors are grateful to this support.

## REFERENCES

- Federal Emergency Management Agency (FEMA), (2007) Raching Protocol for Testing of Nonstructural Components fpr the Purpose of Seismic Performance Assessment, FEMA 461, Washington, D.C.
- Computers and Structures, Inc, (2002) SAP2000 Analysis Reference Manual, Version 8.0, Computers and Structures, Inc., Berkeley
- Timoshenko, Stephen P, Gere, James M (1961) Theory of Elastic Stability, McGraw-Hill, New York
- Chou WJ (2013) A Study on Seismic Capacity of Overhead Transportation Systems in A High-tech Fab, Master Thesis, National Cheng Kung University, Tainan, Taiwan
- Chang YC (2013) A Study on Seismic Behavior and Strengthening of High Slenderness Ratio Braces, Master Thesis, National Cheng Kung University, Tainan, Taiwan